JOURNAL OF SOLID STATE CHEMISTRY 119, 125–130 (1995)

$Lu_3O_2F_5$: A New Highly Densified Member ($n = 3$) of the M_nX_{2n+1} Series of Fluorite-Related Vernier Phases

J. P. Laval,[1] A. Taoudi, A. Abaouz, and B. Frit

Laboratoire de Matériaux Céramiques et Traitements de Surface, URA-CNRS No. 320. Université de Limoges. 123, Avenue A. Thomas, 87060 Limoges Cedex, France

Received August 5, 1994; accepted January 23, 1995

In addition to the nonstoichiometric $LuO_{1-x}F_{1+2x}$ ($0.11 \leq x \leq 0.22$) domain of incommensurate vernier phases, a new stoichiometric phase $Lu_3O_2F_5$ ($x = 0.33$) has been isolated. Its crystal structure has been solved by a Rietveld analysis of its powder X-ray pattern ($R_B = 0.047$). $Lu_3O_2F_5$ crystallizes with orthorhombic symmetry (space group: *Pnma*) and the unit cell parameters $a = 5.544(1)$ Å, $b = 16.875(3)$ Å, $c = 5.292(1)$ Å and $Z = 4$. Its crystal structure can be described as the commensurate member $n = 3$ of the $M_nX_{2n=1}$ series of family I vernier phases, and exhibits the highest anionic rate ever observed in such phases ($MX_{2.33}$). The crystallochemical factors justifying such a surprising anionic densification are analyzed and emphasized. A comparison with Bi_3NF_6, whose structure corresponds to the member $n = 3$ of the series of family II vernier phases, is developed. © 1995 Academic Press, Inc.

INTRODUCTION

The lanthanoide oxyfluorides have been the subject of numerous studies, but until now, the only comprehensive and systematic studies of the LnOF–LnF_3 systems are the works of Abaouz (1) and Taoudi (2). Among other results, these authors confirmed that, for the smallest lanthanoides (Ln = Sm–Lu), the short-range ordered fluorite-related $Ln(O, F)_{2+x}$ phases, observed for Ln = La–Sm (3, 4), were replaced by incommensurate M_nX_{2n+1} vernier phases (5, 6) in which the anionic excess, with respect to the fluorite stoichiometry, is accommodated by a one-dimensional densification process involving the transformation of one-half of the anionic square 4^4 nets into denser hexagonal 3^6 nets (Fig. 1). Ideally, for perfectly regular plane nets with the same spacing, the density of anions in the 3^6 nets is greater than in the 4^4 nets by a factor of $2/\sqrt{3} = 1.1547$, corresponding to $n = 6.46$. In fact, the experimentally observed values of n range from approximately 4 ($MX_{2.25}$) to 9 ($MX_{2.11}$).

Papiernik and Frit (7) have shown that two kinds of fluorite-related vernier phases can be distinguished:

—Type I corresponds to phases containing nearly equivalent quantities of two different anions (lanthanoide oxyfluorides or zirconium nitridefluorides, for example) and in which the densification process extends indefinitely along the same anionic layer (see, for instance, the case of $Y_5O_4F_7$ in Fig. 1c).

—Type II corresponds to phases that contain either only one anion or a majority of one anion, and in which the densification process occurs alternately along each anionic layer, i.e., in which antiphase boundaries divide each anionic layer into alternate 4^4 and 3^6 strips (see, for instance, the case of Dy_5Cl_{11} in Fig. 1d (8)).

Abaouz and Taoudi have also shown that

(i) Whatever the temperature, the extent of the composition range of the $LnO_{1-x}F_{1+2x}$ vernier phases increases from Sm to Lu. For this last element, it corresponds to $0.11 \leq x \leq 0.22$.

(ii) In the case of lutetium, in addition to this nonstoichiometric domain, an original stoichiometric compound $Lu_3O_2F_5$ ($x = 0.33$) exists, whose X-ray pattern exhibits strong analogies with the vernier phases.

This paper deals with the synthesis conditions and the crystal structure of this new compound.

SYNTHESIS AND CRYSTAL STRUCTURE DETERMINATION

$Lu_3O_2F_5$ was prepared by solid state reaction of a suitable mixture of lutetium oxide and fluoride heated for several days in sealed platinum tubes. Whatever the temperature, the composition $LuO_{1-x}F_{1+2x}$, and the annealing time, this phase was never prepared completely pure since small amounts of the vernier phase $Lu(O,F)_{2.22}$ (for $x \leq 0.30$), or LuF_3 (for $x \geq 0.37$), or both impurities (for $0.30 \leq x \leq 0.37$) were always observed. This behavior persists up to 950°C, the temperature at which $Lu_3O_2F_5$ decomposes into LuF_3 and $Lu(O,F)_{2.22}$.

Various attempts to prepare good single crystals of this new compound were unsuccessful. The crystals obtained

[1] To whom correspondence should be addressed.

0022-4596/95 $12.00

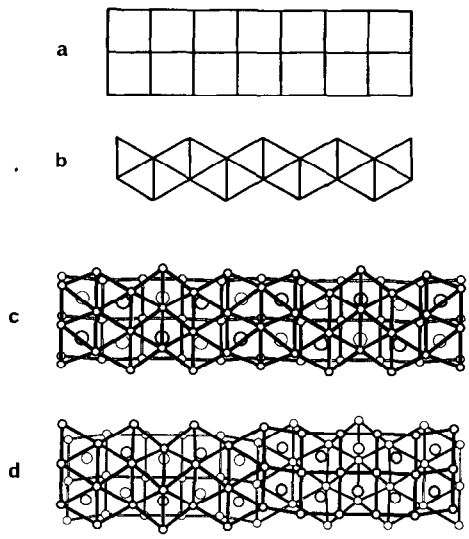

FIG. 1. Accommodation of the anion excess in so-called fluorite-related vernier phases: (a) ideal 4^4 fluorite-like anionic subcell; (b) densified 3^6 anionic subcell; (c) structure of $Y_5O_4F_7$ (n = 5 member type I vernier phase) (6); and (d) structure of Dy_5Cl_{11} (n = 5 member type II vernier phase) (8).

always consisted of a coherent intergrowth of orthorhombic domains characteristic of two distinct fluorite-related superstructures, presenting close a and c parameters, and b parameters that are, respectively, multiples $n = 3$ and $n \approx 5$ of a common basis parameter. The domains with $n \approx 5$ correspond to the limit compound of the "vernier domain," whereas the domains with $n = 3$ correspond to $Lu_3O_2F_5$, whose crystal structure is therefore strongly related to the vernier type.

Accurate analysis of Buerger and Weissenberg pictures of one of these crystals allowed the unambiguous determination of the space group and unit cell parameters of both superstructures:

	a (Å)	b (Å)	c (Å)	Space group
$Lu_5O_4F_7$	5.448(1)	5 × 5.449(1)	5.297(1)	*C2mb* or *Cmmb*
$Lu_3O_2F_5$	5.544(1)	3 × 5.625(1)	5.292(1)	*Pnma*

We can see that if the c parameters are nearly identical, the a and b parameters of the subcell are greater for $Lu_3O_2F_5$. This behavior is in accordance with what is commonly observed in the vernier series.

The quality of these crystals did not allow further knowledge of the crystal structure of $Lu_3O_2F_5$, so we decided to determine it by a Rietveld analysis of the powder X-ray diffraction pattern.

The sample selected corresponded to an overall composition $Lu(O,F)_{2.37}$ and contained ≈5 mole% $Lu(O,F)_{2.22}$ and ≈10 mole% LuF_3. The synthesis process included heating at 900°C for 1 day, grinding in an agate mortar, annealing for 2 days at 850°C, and then water quenching. The sample holder was filled on its lateral side by the finely ground and sieved powder, in order to avoid preferential orientation of the crystallites.

The powder X-ray pattern was recorded on a Siemens D5000 diffractometer under the conditions given in Table 1. The structure determination was carried out with the programs Arit4 (9) and Fullprof (10) by simultaneously refining the structural parameters of $Lu_3O_2F_5$ and impurities. The structure of LuF_3 was extrapolated from that of YbF_3 (11) and that of the incommensurate $Lu(O,F)_{2.22}$ simulated by that of $Y_5O_4F_7$ (6). The closeness of the subcells of $Lu(O,F)_{2.22}$ and $Lu_3O_2F_5$ led to severe problems of peak overlapping and the refinement process was possible only by using a pseudo-Voigt function and a progressive release of variables.

In a first step, two cationic sites Lu(1) and Lu(2) were detected by analysis of Patterson maps calculated after a profile-fitting process applied to the experimental X-ray pattern (Aritb option of the Arit4 program). After refinement of these sites, four anionic sites were identified on Fourier-difference maps and then refined. Numerous refinement cycles alternating with manual adjustments of the background and refinement of the two impurities led to a good approach of the $Lu_3O_2F_5$ crystal structure (R_B = 4.7%). In order to avoid an excessive number of variables, neither anisotropic components of the temperature factors nor preferential orientation corrections were introduced during the final step of the refinement

TABLE 1
Crystal Data and Conditions of Recording and Refinement

Space group	*Pnma*
Unit cell parameters (Å)	a = 5.544(1)
	b = 16.875(3)
	c = 5.292(1)
	Z = 4
Measurement range (2θ)	15–126°
Wavelength	Cu$K\alpha$(1.540598 Å)
	Graphite back monochromator
Step (2θ)	0.04°
Zero shift (2θ)	0.021°
Number of reflections	412
Number of refined parameters	33
Profile parameters	U = 0.012(1)
	V = −0.004(1)
	W = 0.0076(4)
	η = 0.71(1)
Final refinement program	Fullprof
Profile function	Pseudo-Voigt
R factors (%)	R_B = 4.7
	R_P = 8.9
	R_{WP} = 11.5

TABLE 2
Refined Structural Parameters for $Lu_3O_2F_5$ (Standard Deviations between Brackets)

Atom	Site	Coordinates			B (Å^2)
Lu(1)	4*c*	0.7621(2)	1/4	0.0427(3)	0.07(4)
Lu(2)	8*d*	0.1750(2)	0.5973(1)	0.5380(2)	0.13(3)
O	8*d*	0.043(2)	0.3254(7)	0.202(2)	0.8(3)
F(1)	8*d*	0.119(2)	0.4858(7)	0.291(2)	0.8(3)
F(2)	8*d*	0.337(2)	0.8731(6)	0.180(2)	0.8(3)
F(3)	4*c*	0.400(3)	1/4	0.856(3)	0.8(3)

with Fullprof program, and all anions were constrained to have the same thermal coefficient.

The refined structural parameters are given in Table 2, and the main interatomic distances in Table 3. The experimental, calculated, and difference patterns are shown in Fig. 2.

DESCRIPTION OF THE STRUCTURE AND DISCUSSION

In order to determine if anionic ordering was effective in this phase as in numerous fluorite-related oxyfluorides, the electrostatic bond valence was calculated for each anion by using Brown's method (12, 13). The results are as follows:

Site	Coordination	Bond Valence	
		calc.	theor.
O	4	2.07	2
F(1)	3	0.96	1
F(2)	3	1.04	1
F(3)	2 + 2	0.92	1

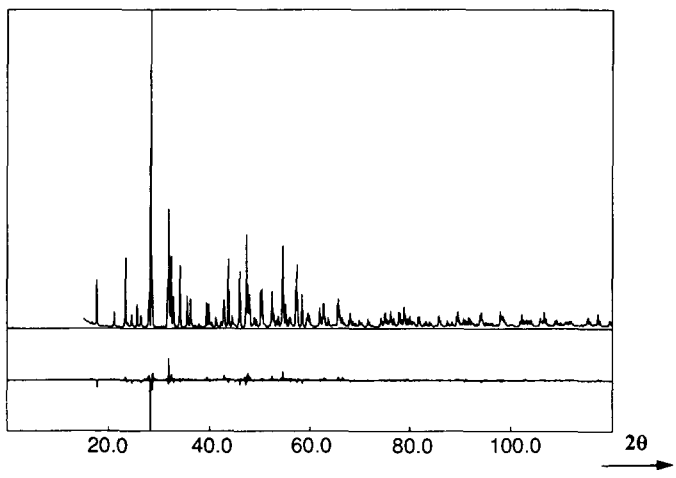

FIG. 2. Observed (dotted lines), calculated (solid lines), and difference (bottom) X-ray powder diffraction patterns for $Lu_3O_2F_5$. Note: dotted lines are exactly superposed on solid lines.

TABLE 3
Selected Bond Lengths (Å)

	Distances (Å)		Distances (Å)
		Lu(2)–Lu(2)	3.566(2)
Lu(1)–Lu(1)	3.535(2)		4.120(2)
	4.157(2)		3.836(2)
			4.299(3)
Lu(1)–Lu(2)	4.026(2)		
	3.537(2)	Lu(2)–O	2.25(1)
	3.418(2)		2.21(1)
	4.047(2)		
		Lu(2)–F(1)	2.31(1)
Lu(1)–O	2.18(1) × 2		2.33(1)
	2.22(1) × 2		2.25(1)
Lu(1)–F(2)	2.45(1) × 2	Lu(2)–F(2)	2.16(1)
			2.26(1)
Lu(1)–F(3)	2.24(1)	Lu(2)–F(3)	2.78(1)
	2.24(1)		
O–O	2.54(2)	F(1)–F(1)	2.62(2)
O–F(1)	2.78(2)	F(1)–F(2)	2.73(2)
O–F(2)	2.74(2)	F(2)–F(3)	2.63(2)
O–F(3)	2.78(2)	F(2)–F(3)	2.55(1)

They clearly indicate that F and O atoms are strictly ordered, with the oxygen atoms logically occupying the anionic site of higher coordination. In addition, the good agreement between theoretical and experimental values confirms the validity of the structural determination despite the unfavorable experimental conditions of the refinement.

Figures 3a and 3b show projections of the $Lu_3O_2F_5$ structure onto xy and yz planes, respectively, and Fig. 4 gives a stereoview of the coordination polyhedra around each individual cation.

Lu(1) (Fig. 4a) is surrounded by eight anions (4 O at distances 2.18–2.22 Å and 4 F at distances ranging from 2.24 to 2.45 Å) forming a polyhedron which can be described:

—Either as a distorted square antiprism (4 oxygen atoms forming the nearly planar first square face, and 2 F(1) and 2 F(2) forming the very distorted second one),

—or, more relevantly, as a bicapped trigonal prism (F(2) being the capping anions).

Lu(2) is surrounded by seven anions (5 F and 2 O (Fig. 4b)) forming a very distorted monocapped trigonal prism, similar to the ZrO_7 anionic polyhedron observed in the α-ZrO_2 baddeleyite structure. An eighth anion, F(3), is located at a longer distance (2.78 Å) from Lu(2), whose coordination can then be considered as [7 + 1] (irregular bicapped trigonal prism).

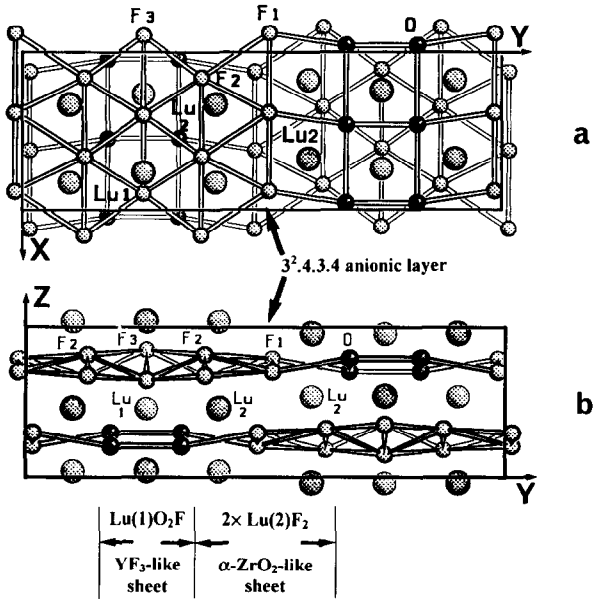

FIG. 3. Projections of the $Lu_3O_2F_5$ structure onto the (a) *xy* and (b) *yz* planes.

$Lu_3O_2F_5$ clearly exhibits the main structural features of vernier phases, especially:

—A distorted fcc cationic array within which Lu–Lu distances are in the range 3.42–4.30 Å (Fig. 5).

—Parallel and alternate 3^6 and 4^4 strips containing, respectively, four and three [100] anionic rows. However, in contrast to the other $LnO_{1-x}F_{1+2x}$ vernier phases which belong to family I, $Lu_3O_2F_5$ can be considered the $n = 3$ member of family II. Such a member, which corresponds to an abnormally high densification of the anionic subcell (overall composition $MX_{2.33}$) had never been identified since the largest composition range observed for the M_nX_{2n+1} vernier phases corresponds to $MX_{2.11}$–$MX_{2.25}$, i.e., $4 \leq n \leq 9$.

In this kind of phase, the densification of the anionic subcell, with respect to the parent fluorite structure, and the corresponding layer mismatch cause severe sterical constraints which are relieved by:

—A systematic more-or-less important distortion of the fcc cationic array and a puckering of the 3^6 anionic layers;

—a partial ordering of anions in the case of family I phases (the smaller and less-charged anions occupy the densified 3^6 layers); and

—the formation of periodic antiphase boundaries in the case of family II phases.

The surprisingly high densification in the $Lu_3O_2F_5$ structure is made possible by the quasi-unique conjunction of all these factors:

—A densification mode of type II, which, by the formation of periodic antiphase boundary planes, allows the strain energy to be reduced;

—a full O/F order in which oxide anions are strictly located in the square 4^4 strips, whereas fluoride anions constitute the densified 3^6 strips and the antiphase boundaries (Fig. 3);

—a puckering of the anionic layers (mainly in the 3^6 strips—see Fig. 3b) which, as in the yttrium oxyfluorides

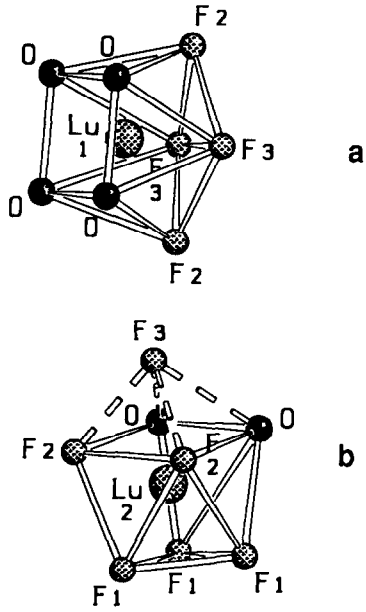

FIG. 4. Cation coordination polyhedra in the $Lu_3O_2F_5$ structure (a) $Lu(1)O_4F_4$ bicapped trigonal prism and (b) $Lu(2)O_2F_5$ monocapped trigonal prism.

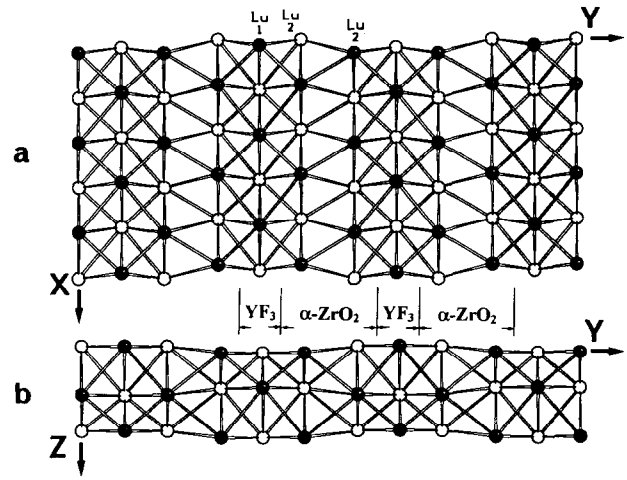

FIG. 5. Projection of the cationic network onto (a) *xy* and (b) *yz* planes.

but at a higher degree, deviate from planeity, thus increasing the possibilities of densification;

—a very important distortion of the cationic subcell (Fig. 5) which in the neighboring of the antiphase boundaries is closer to the baddeleyite-type cationic subcell observed in the monoclinic LuOF compound (14) than to a fluorite-type one.

Considering this last point and the fact, clearly shown by the *yz* projection of Fig. 3b, that the anions in excess of those in the fluorite-type schematically correspond to zigzag [001] rows of F(3) anions inserted within the Lu(1) planes, the $Lu_3O_2F_5$ structure can then be described as a coherent intergrowth along the superstructure axis O*y*, in the ratio 2/1, of parallel $Lu(2)F_2$ and $Lu(1)O_2F$ sheets, respectively, with the same level for α-ZrO_2 baddeleyite and YF_3-type structures (Figs. 3 and 5). With a similar approach, the $Nb_2Zr_6O_{17}$ crystal structure (member $n = 8$ of the family II vernier phases) has already been described as being composed of layered unit cells of $Y_7O_6F_9$ type, in antiphase and interspersed with unit lamellae of the same level for α-PbO_2-type (5, 15).

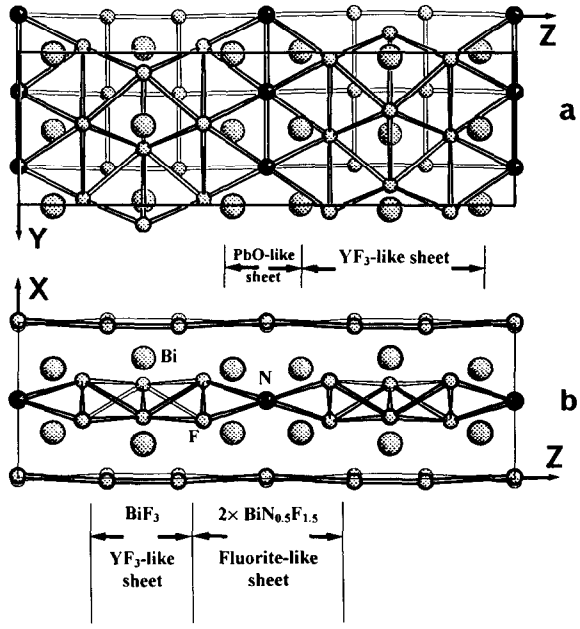

FIG. 6. Projections onto the (a) *yz* and (b) *xz* planes of the Bi_3NF_6 structure.

COMPARISON WITH THE Bi_3NF_6 STRUCTURE

Within the context of a common French–German research program on nitridefluoride compounds, the crystal structure of a new bismuth nitridefluoride Bi_3NF_6 was recently solved (16) (Fig. 6), presenting great analogies with the $Lu_3O_2F_5$ structure, which makes a detailed comparison interesting.

Both phases:

—are strictly stoichiometric, with the same $MX_{2.33}$ overall composition;

—have a strictly ordered anionic subcell; and

—are closely related to the M_nX_{2n+1} series of fluorite-related vernier phases, series of which can be considered highly densified $n = 3$ members.

However, in contrast to $Lu_3O_2F_5$, Bi_3NF_6 does not contain antiphase boundaries and so belongs to family I of the vernier phases. Therefore, the high anionic densification and the corresponding constraints are now accommodated, in addition to the "classical" strong puckering of the anionic 3^6 layers, mainly by an original anionic ordering: the N atoms are periodically distributed within the densified 3^6 layers as infinite [010] chains of NBi_4 tetrahedra sharing Bi–Bi edges and which, thanks to strong and therefore short (≈2.25 Å) covalent Bi–N bonds, stabilize the structure.

It is highly probable, in addition, that the great crystallochemical adaptability of the Bi^{3+} cations also plays an important role in the stabilization of such a structure, which presupposes a progressive evolution of the cation coordination along the superstructure axis. It is significant from this point of view to note that in the homologous fluorite-related lanthanoide nitridefluorides, the excess of anions is accommodated by finite 1:0:3 clusters rather than by an infinitely adaptive process like the vernier process (17). In the same type of scheme as for $Lu_3O_2F_5$, the Bi_3NF_6 structure can be described as a regular succession along the *Oz* superstructure axis, and still in the ratio 2/1, of parallel $BiN_{0.5}F_{1.5}$ and BiF_3 sheets with, respectively, the fluorite- and the YF_3-type structures. The change from α-ZrO_2 to fluorite in the MX_2 sheets, clearly evidenced by the two projections in Fig. 7, simply results from the disappearance of the antiphase boundaries in Bi_3NF_6. This allows the anionic layers of the corresponding planes to remain of the 4^4 fluorite type, i.e., not to transform as in $Lu_3O_5F_2$ into a corrugated $3^2.4.3.4$ layer, characteristic of the α-ZrO_2 baddeleyite structure. It is also worth pointing out that, because of the shortening of the distances between Bi *xy* planes sandwiching the mixed NF anionic layers in Bi_3NF_6, with respect to the corresponding distances between Lu(2) *xz* planes sandwiching the F(1) $3^2.4.3.4$ layers in $Lu_3O_2F_5$ (see Figs. 3b and 6b), the Bi_3NF_6 structure can be considered composed of YF_3-like sheets regularly separated by $BiN_{0.5}F_{0.5}$ lamellae with PbO-like structure.

CONCLUSION

Once more the fundamental role played by anion ordering in the accommodation of the excess of anions in

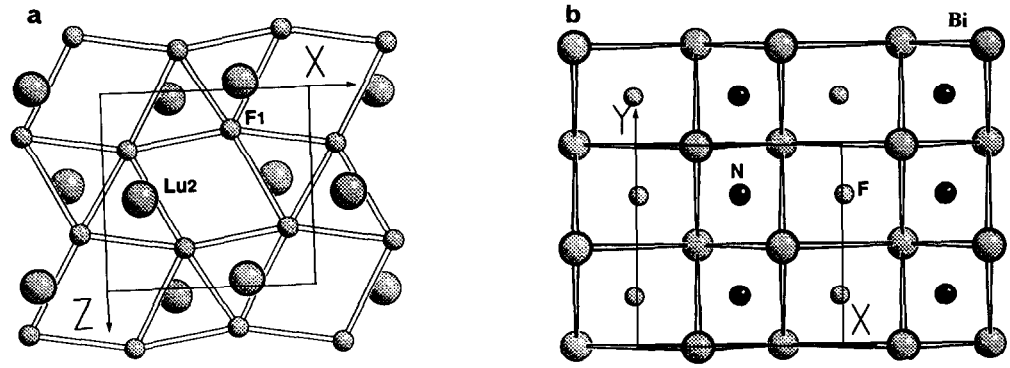

FIG. 7. (a) [010] Projection of the central part of the α-ZrO_2-type sheet in $Lu_3O_2F_5$, showing a $3^2.4.3.4$ F(1) anionic layer sandwiched between two Lu(2) cationic layers. (b) [001] Projection of the distorted (small and large NBi_4 and FBi_4 tetrahedra, respectively) PbO-like sheet in Bi_3NF_6.

mixed-anion fluorite-related phases is emphasized. Moreover, the Bi_3NF_6 and $Lu_3O_2F_5$ structures clearly demonstrate that, thanks to the anion ordering but at the expense of strict stoichiometric conditions and with a correlative loss of their infinitely adaptive character, vernier phases with an "abnormally" high degree of anionic densification can be stabilized.

It is evident that a careful and systematic analysis of the anionic distribution in mixed-anion phases can be a powerful guide for the prediction and then the synthesis of new interesting compounds.

REFERENCES

1. A. Abaouz, Thesis, University of Limoges, 1988.
2. A. Taoudi, Thesis, University of Limoges, 1992.
3. J. P. Laval, A. Abaouz, B. Frit, G. Roult, and W. T. A. Harrison, *Eur. J. Solid State Inorg. Chem.* **25,** 425 (1988).
4. J. P. Laval, A. Abaouz, B. Frit, and A. Le Bail, *Eur. J. Solid State Inorg. Chem.* **27,** 545 (1990).
5. B. G. Hyde, A. N. Bagshaw, S. Andersson, and M. O'Keeffe, *Annu. Rev. Mater. Sci.* **4,** 43 (1974).
6. D. J. M. Bevan, J. Mohyla, B. F. Hoskins, and R. J. Steen, *Eur. J. Solid State Inorg. Chem.* **27,** 451 (1990).
7. R. Papiernik and B. Frit, *Acta Crystallogr. Sect. B* **42,** 342 (1986).
8. H. Bärnighausen, *in* "Proceedings, 12th Rare Earth Research Conference" (C. E. Lundin, Ed.), Vol. 1, p. 404, 1976.
9. A. Le Bail, H. Duroy, and J. L. Fourquet, *Mater. Res. Bull.* **23,** 447 (1988).
10. L. Rodriguez-Carvajal, "Fullprof", version 2.2, I.L.L. program. Grenoble, June 1992.
11. B. V. Butveskii and L. S. Garashina, *Koord. Khim.* **3,** 1024 (1977).
12. I. D. Brown, "Structure and Bonding in crystals" (M. O'Keeffe and A. Navrotsky, Eds.), New York, Academic Press, (1981).
13. I. D. Brown and D. Altermatt, *Acta Crystallogr. Sect. B* **41,** 244 (1985).
14. A. Taoudi, J. P. Laval, and B. Frit, *Mater. Res. Bull.* **29,** 1137 (1994).
15. J. Galy and R. S. Roth, *J. Solid State Chem.* **7,** 277 (1973).
16. M. Hofman, E. Schweda, J. Strähle, J. P. Laval, B. Frit, and M. A. Estermann, *J. Solid State Chem.* **119,** 73 (1995).
17. T. Vogt, E. Schweda, J. P. Laval, and B. Frit, *J. Solid State Chem.* **83,** 324 (1989).